

Absorption, quenching, and enhancement by tracer in acetone/toluene laser-induced fluorescence

Guang Chang(常光), Xin Yu(于欣), Jiangbo Peng(彭江波), Yang Yu(于杨), Zhen Cao(曹振), Long Gao(高龙), Minghong Han(韩明宏), and Guohua Wu(武国华)

Citation: Chin. Phys. B, 2020, 29 (**12**): 124212. DOI: 10.1088/1674-1056/abb3e1
Journal homepage: http://cpb.iphy.ac.cn; http://iopscience.iop.org/cpb

What follows is a list of articles you may be interested in

High efficiency sub-nanosecond electro-optical *Q*-switched laser operating at kilohertz repetition frequency

Xin Zhao(赵鑫), Zheng Song(宋政), Yuan-Ji Li(李渊骥), Jin-Xia Feng(冯晋霞), Kuan-Shou Zhang(张宽收)
Chin. Phys. B, 2020, 29 (**8**): 084205. DOI: 10.1088/1674-1056/ab8ac4

Gain-induced large optical torque in optical twist settings

Genyan Li(李艮艳), Xiao Li(李肖), Lei Zhang(张磊), Jun Chen(陈君)
Chin. Phys. B, 2020, 29 (**8**): 084201. DOI: 10.1088/1674-1056/ab9616

Optical nonreciprocity in a piezo-optomechanical system

Yu-Ming Xiao(肖玉铭), Jun-Hao Liu(刘军浩), Qin Wu(吴琴), Ya-Fei Yu(於亚飞), Zhi-Ming Zhang(张智明)
Chin. Phys. B, 2020, 29 (**7**): 074204. DOI: 10.1088/1674-1056/ab8abf

A low-noise, high-SNR balanced homodyne detector for the bright squeezed state measurement in 1-100 kHz range

Jin-Rong Wang(王锦荣), Qing-Wei Wang(王庆伟), Long Tian(田龙), Jing Su(苏静), Yao-Hui Zheng(郑耀辉)
Chin. Phys. B, 2020, 29 (**3**): 034205. DOI: 10.1088/1674-1056/ab683b

Quantitative measurements of one-dimensional OH absolute concentration profiles in a methane/air flat flame by bi-directional laser-induced fluorescence

Yu Xin, Yang Zhen, Peng Jiang-Bo, Zhang Lei, Ma Yu-Fei, Yang Chao-Bo, Li Xiao-Hui, Sun Rui
Chin. Phys. B, 2015, 24 (**11**): 114204. DOI: 10.1088/1674-1056/24/11/114204

Absorption, quenching, and enhancement by tracer in acetone/toluene laser-induced fluorescence*

Guang Chang(常光)[1,2], Xin Yu(于欣)[1,2], Jiangbo Peng(彭江波)[1,2,†], Yang Yu(于杨)[1,2], Zhen Cao(曹振)[1,2], Long Gao(高龙)[1,2], Minghong Han(韩明宏)[1,2], and Guohua Wu(武国华)[1,2]

[1] *National Key Laboratory of Science and Technology on Tunable Laser, Harbin Institute of Technology, Harbin* 150080, *China*
[2] *Institute of Opto-Electronics, Harbin Institute of Technology, Harbin* 150080, *China*

(Received 23 May 2020; revised manuscript received 28 August 2020; accepted manuscript online 1 September 2020)

To measure the equivalent ratio distribution of the two-stage lean premixed (DLP) flame, we propose using acetone/toluene planar laser-induced fluorescence (PLIF) technology to simultaneously measure the concentrations of the two components. Appropriate excitation laser wavelength and filters are used to assess the influence of acetone and toluene on each other's fluorescence signal at room temperature. Experimental results show that acetone has a strong absorption effect on toluene's fluorescence signal, the effective absorption cross-section is 5.77×10^{-20} cm^{-2}. Acetone has an obvious quenching effect on the toluene fluorescence signal, and the Stern–Volmer coefficient is 0.50 kPa^{-1}. The collisions between the molecules of toluene and acetone will lead to the enhancement of the fluorescence signal of acetone, and the enhancement coefficient is exponential with the acetone's concentration. The quantitative relationship between the fluorescence intensity and the concentrations of the two tracers is obtained by establishing the photophysical model of toluene and acetone's fluorescence signals.

Keywords: laser-induced fluorescence, two tracers, absorption cross-section, fluorescence quantum yield

PACS: 42.62.Fi **DOI:** 10.1088/1674-1056/abb3e1

1. Introduction

Due to the increasingly serious air pollution, combustion emissions have become a topic of concern.[1] Lean premixed (LP) combustion is a common method of reducing NO_x.[2,3] However, low equivalent ratio flames are easily flameout.[4,5] Zhao[6] studied dual-stage lean premixed (DLP) flame combustion by configuring two lean premixed gases with different equivalent ratios to achieve stable flame combustion. The most important feature of the DLP is the multiscale distribution of the input equivalence ratio. Studies have reported that the flames propagating in varying equivalence ratio zones clearly differ from equivalent homogeneous flames,[7–10] so the equivalent ratio distribution measurement has guiding significance for improving the DLP. Since the respective equivalent ratios of the two gases are known, a technique is required that can simultaneously quantitatively measure concentrations of both. Although most flames in industrial combustors are turbulent, the research should start from the laminar flow field at room temperature and normal pressure to avoid the influence of turbulent fluctuations and capture more accurate concentration distribution data. Therefore, the measurement object of this study is the flow field under room temperature and normal pressure.

Traditional sensor probe measurement technology is difficult to obtain the original structure of the flow field, resulting from the interference of intrusive detection. As a diagnostic technique, the optical measurement technique plays an important role in the flow field analysis at present. The greatest advantage of the optical measurement is a completely non-contact measurement without destroying the original structure of the flow field. The tunable diode-laser absorption spectroscopy (TDLAS), laser-induced breakdown spectroscopy (LIBS), coherent anti-stokes Raman spectroscopy (CARS), and other laser spectral measurement technologies have high measurement accuracy.[11–15] However, these laser spectral measurement technologies work only with a few single points or single lines. The planer laser-induced fluorescence (PLIF) is a non-contact imaging technique for concentration distribution measurements of the liquid and gaseous flow field in a two-dimensional plane,[16–18] which is particularly suitable for measuring the concentration of the whole flow field. The PLIF technology can select two tracers to represent two different gas components to achieve the measurement target for the flow field of the DLP.

To measure the two components' concentration, detectors simultaneously capture the fluorescence signals of corresponding tracers, and shield the other fluorescence signals. This requires a large difference in the peak fluorescence spectrum of the two tracers. Ketone compounds represented by acetone[19–22] and 3-pentanone[23,24] and aromatic compounds represented by toluene[25–28] are both widely used as the PLIF tracers. Among these tracers, the fluorescence spectrum's peak regions of acetone and toluene are far away from each

*Project supported by the National Natural Science Foundation of China (Grant Nos. 51536002, 61405048, and 91441130).
†Corresponding author. E-mail: pengjiangbo_2004@126.com
© 2020 Chinese Physical Society and IOP Publishing Ltd

other, which are very suitable for the simultaneous concentration measurement of two components. Compared with the same type of tracers, acetone and toluene have higher saturated vapor pressure, which is suitable for the concentration measurement of the gaseous flow field. Relying on the characteristic that the fluorescence signals of NO and acetone are easy to distinguish, Meyer[29] used the NO/acetone dual tracer PLIF technology to realize the visualization of the two gas components' mixing process. However, NO is a toxic gas that can be hazardous in engineering applications. Since the wavelengths of the lasers used to excite nitric oxide and acetone differ, this PLIF system requires a variety of lasers, including tunable lasers that can excite NO. This greatly increases the complexity of the laser system. The research results of Thurber[22] and Koban[25] showed that under room temperature conditions, both the absorption spectra of acetone and toluene contain a region that overlaps each other, and a single wavelength laser can simultaneously excite th two tracers. Toluene and acetone are relatively non-toxic and safe, suitable for open flow field measurement. Therefore, this study selects acetone and toluene as the tracers.

Previous research results[21,30] indicate that under the conditions of determining the excitation laser wavelength and the filter, the temperature, pressure, and gas composition have a significant effect on acetone and toluene's absorption cross-section and fluorescence quantum yield (FQY). The measurement object of this study is the atmospheric pressure flow field at room temperature, so the influence of pressure and temperature can be excluded. In order to minimize the influence of various gas compositions on the fluorescence intensity, only nitrogen is used to dilute acetone and toluene in the following experimental studies. Thus, the main non-concentration factor that affects the tracers' fluorescence intensity is the effect of acetone and toluene on each other's fluorescence signals.

This paper validates the feasibility of using acetone/toluene PLIF technology to achieve the simultaneous measurement of two gas components' concentration. The absorption spectra and fluorescence spectra characteristics of acetone and toluene are studied to assess the appropriate excitation wavelength and filter, respectively. The influence of the tracers on each other is quantitatively assessed in a static cell, and a photophysical model is obtained that provides the quantitative relationship between the components' concentrations and respective fluorescence intensity.

2. Theoretical background

Assuming constant filtering, constant detector gain, and identical collection optics, in the normal pressure and room temperature flow field, the fluorescence signal intensity of a single tracer at a certain position can be expressed by

$$S_{\mathrm{lif}} = kE(x)n_{\mathrm{tracer}}(x)\sigma(\lambda_{\mathrm{ex}})\phi(\lambda,\lambda_{\mathrm{ex}},n_{\mathrm{i}}(x)), \tag{1}$$

where x is the position of the observation point, which is determined by the laser transmission distance in the tracer vapor. $E(x)$ is the laser energy density used to excite the tracer. $n_{\mathrm{tracer}}(x)$ is tracer's concentration. $\sigma(\lambda_{\mathrm{ex}})$ is the absorption cross-section of the tracer under an incident light wavelength of λ_{ex}. $\phi(\lambda,\lambda_{\mathrm{ex}},n_{\mathrm{i}}(x))$ is the FQY of the tracer molecule determined by the concentration of compositions $n_{\mathrm{i}}(x)$, excitation laser wavelength λ_{ex}, and specific fluorescence wavelength λ. k is the calibration constant.

After determining the excitation laser wavelength and filter, equation (1) can be simplified to

$$S_{\mathrm{lif}} = kE(x)n_{\mathrm{tracer}}(x)\sigma\phi(n_{\mathrm{i}}(x)). \tag{2}$$

According to Lambert–Beer's law, $E(x)$ can be expressed by

$$E(x) = E_0 \exp\left(-\int_0^x \sigma n_{\mathrm{tracer}}(x)\,\mathrm{d}x\right), \tag{3}$$

where E_0 is the laser energy density at $x = 0$.

This study uses a static cell with a constant volume. Tracer vapor and various diluent gases are considered ideal gases, so the partial pressure (kPa) of a certain component is used to represent its concentration. The concentration of each gas component is consistent everywhere inside the static cell. And there is only a diluent gas of nitrogen inside the static cell, so equations (2) and (3) can be further developed into

$$S_{\mathrm{lif}} = kE_0 \exp(-\sigma n_{\mathrm{tracer}}x)n_{\mathrm{tracer}}\sigma\phi(n_{\mathrm{N_2}},n_{\mathrm{tracer}}). \tag{4}$$

Since the measurement object is the normal pressure flow field, the total pressure inside the static cell is 101 kPa. In this study, the partial pressure of nitrogen ranges from 90 kPa to 101 kPa, and the effect of nitrogen on the FQY of acetone and toluene is negligible. According to the research results of Hartwig,[20] when the tracer vapor concentration is low, the higher molecular collision efficiency and faster vibration relaxation rate caused by the increased tracer concentration can also be neglected. In this way, the FQY can be considered as constants, and equation (4) can be further simplified as

$$S_{\mathrm{lif}} = kE_0 \exp(-\sigma n_{\mathrm{tracer}}x)n_{\mathrm{tracer}}\sigma. \tag{5}$$

When the excitation laser energy ($E\exp(-\sigma n_{\mathrm{tracer}}x)$) is normalized, the tracer concentration and its fluorescence intensity approximated have a linear relationship. This is the basic principle of single tracer LIF technology to achieve flow field concentration measurement. But when there are two tracers besides nitrogen in the flow field, acetone and toluene, then equation (5) can be further developed into the following ones:

$$S_{\mathrm{t}} = k_{\mathrm{t}}E_0 \exp(-(\sigma_{\mathrm{a}}n_{\mathrm{a}} + \sigma_{\mathrm{t}}n_{\mathrm{t}})x)n_{\mathrm{t}}\sigma_{\mathrm{t}}\frac{\phi_{\mathrm{t}}(n_{\mathrm{a}})}{\phi_{\mathrm{t}}(n_{\mathrm{a}}=0\ \mathrm{kPa})}T_{\mathrm{t}}(n_{\mathrm{a}}), \tag{6}$$

$$S_{\mathrm{a}} = k_{\mathrm{a}}E_0 \exp(-(\sigma_{\mathrm{a}}n_{\mathrm{a}}+\sigma_{\mathrm{t}}n_{\mathrm{t}})x)n_{\mathrm{a}}\sigma_{\mathrm{a}}\frac{\phi_{\mathrm{a}}(n_{\mathrm{t}})}{\phi_{\mathrm{a}}(n_{\mathrm{t}}=0\ \mathrm{kPa})}T_{\mathrm{a}}(n_{\mathrm{t}}), \tag{7}$$

where S_t, n_t, σ_t, and k_t represent the fluorescence intensity, concentration, absorption cross-section, and calibration constant of toluene, respectively. $\phi_t(n_a)/\phi_t(n_a = 0\ \text{kPa})$ represents the variation coefficient of toluene's FQY due to the presence of acetone with a concentration of n_a. $T_t(n_a)$ is the transmittance of the toluene's fluorescence signal. This is because toluene's fluorescence signal will be partially absorbed by acetone with a concentration of n_a in the environment before reaching the detector. The same naming rules also apply to acetone. The tracers' effective absorption cross-section on each other's fluorescence signals can be calculated by Lambert–Beer's law. The variation coefficient of the FQY needs to study the changing trend of the tracer's fluorescence intensity after being affected by the other tracer.

The effect of the two tracers, acetone and toluene, on each other's fluorescence signal intensity is mainly reflected in the quenching and enhancement of the fluorescence intensity. Take the acetone's effect on toluene as an example, I_0 is the toluene's fluorescence intensity without acetone, and I is the toluene's fluorescence intensity after being affected by acetone. $n(T)$ is acetone's concentration. Therefore, I/I_0 is the variation coefficient of toluene's FQY. If acetone has quenching effect on toluene's fluorescence, the strength of quenching effects is analyzed using the Stern–Volmer equation

$$\frac{I_0 - I}{I} = k_{SV} \times n(T) = \frac{I_0}{I} - 1. \tag{8}$$

The Stern–Volmer coefficient k_{SV} represents the quenching ability of acetone to toluene's fluorescence signal. If acetone has an enhancement effect on toluene's fluorescence, we can use k_G in the following equation to evaluate the enhancement ability of acetone to toluene's fluorescence signal:

$$\frac{I - I_0}{I_0} = k_G \times n(T) = \frac{I}{I_0} - 1. \tag{9}$$

By studying the variation trend of I/I_0, we can quantify the variation coefficient of the FQY. The toluene's effect on acetone can also be analyzed in this way.

3. Experiment

3.1. Fluorescence detection

An optically-accessible static cell provides this experiment's research environment. The cell has quartz glass windows on four sides for the incident of UV pulsed laser and acquisition of fluorescence signals, and the inside is a cube with a side length of 13 cm. The gas path structure of the static cells is shown in Fig. 1. Open the No. 1 needle valve and use a mechanical pump to pump the pressure inside the static cell below 0.05 kPa. Then close the No. 1 needle valve. The mechanical pump is used to remove air from a stainless steel tank containing liquid acetone, then the tank's ball valve is closed. After 20 minutes, the pressure inside the tank is stabilized, and the pressure is the acetone's saturated vapor pressure at the temperature inside the tank. The tank contains only acetone vapor. Pure toluene vapor can be obtained in the same way. Open the No. 3 needle valve, and the pure toluene vapor flows into the static cell slowly under the control of the needle valve. The vacuum gauge can measure the partial pressure of toluene vapor in the static cells in real-time. When the partial pressure of toluene reaches the requirement, close the No. 3 needle valve. Open No. 2 needle valve, because the saturated vapor pressure of acetone at room temperature is much higher than that of toluene, and pure acetone vapor will flow into the static cells slowly under the control of the needle valve. When the partial pressure of acetone reaches the requirement, close the No. 2 needle valve. Open the No. 1 needle valve, nitrogen flows into the static cell at a fast speed. We use the pressure meter to measure the variation of the total pressure in real-time. When the total pressure is higher than 90 kPa, the needle valve is used to reduce the nitrogen flow rate, so that the total pressure can reach 101 kPa slowly.

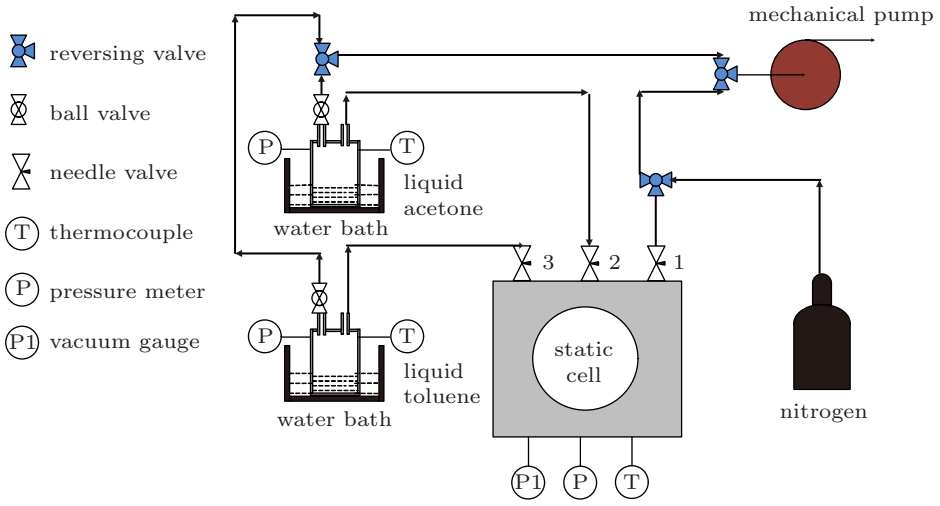


Fig. 1. The gas path structure of static cells.

The frequency of the pulse laser is 1 Hz. The transmitted light energy has a linear relationship with the reflected light energy after the laser pulse incidents onto a quartz plate at 45°. This relationship is used to monitor the incident pulse laser energy by placing a quartz plate in front of the cell. A laser energy meter probe is placed behind the cell to measure the pulsed laser's residual energy. The position where the pulsed laser enters and leaves the static cell is in the center of the two windows. Laser-induced fluorescence from the center of the cell is collected by a spectrometer or an Andor ICCD, so the x in Eq. (5) is 6.5 cm. A schematic of the experiment is shown in Fig. 2. The timing control of the experimental systems is coordinated by the Stanford research system, DG546.

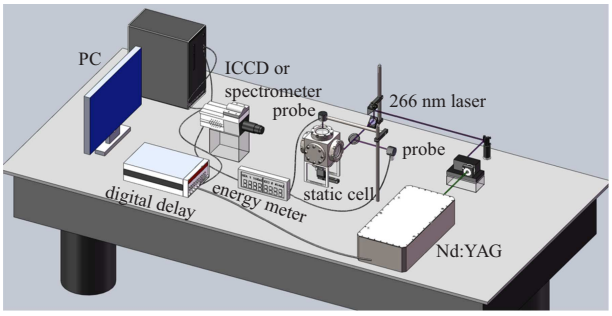


Fig. 2. Schematic of the tracer fluorescence acquisition experiment.

According to Thurber's[21] research, the main error of the static cell experiment comes from three aspects: the adsorption of tracer vapor by the wall, the insufficient mixing of nitrogen and tracer vapor, and the photolysis of the tracer caused by the laser. The needle valve is used to make the tracer vapor slowly fill into the static cells, and the dynamic balance of adsorption and desorption is achieved during this process in the static cell. Nitrogen can flow into the static cells at a fast speed and be fully mixed with the tracer vapor inside. When the internal pressure approaches 101 kPa, reduce the nitrogen flow rate. The time interval between configuring the experiment gas and the LIF experiment needs to exceed 5 minutes. This ensures the full mixing of nitrogen and tracer vapor. The trigger signal of the DG645 comes from the ICCD. Only when the ICCD is working, the laser will run. In this study, the number of ICCD acquisitions for each working condition is 40, and the laser shot number is also 40. The laser energy density range in this experiment is 13–64 mJ/cm^2. The tracer photolysis effect caused by such laser shot number and laser energy density is negligible.

3.2. Absorption effect detection

The absorption effects of two tracers on each other's fluorescence signal are studied based on the experiment in Fig. 3. The absorption cell is placed between the ICCD and the static cell. One tracer is injected into the absorption cell, and the other tracer is injected into the static cell. The fluorescent signal in the static cell has to pass through the absorbent cell to be collected by the ICCD. Thus, as the partial pressure of the tracer in the absorption cell changes, the variations in the fluorescence intensity in the static cell occur, and the absorption effect of one tracer on the fluorescence signal of the other tracer is obtained. When the absorption spectroscopy is conducted on this platform, the static cell is replaced with deuterium lamps, the ICCD is replaced by a spectrometer, and no laser equipment is required. Light with a stable spectrum emitted by the deuterium lamp will pass through the absorption cell and enter the spectrometer. According to the spectral change caused by the tracer's concentration change in the absorption cell, the tracer's absorption spectrum is obtained.

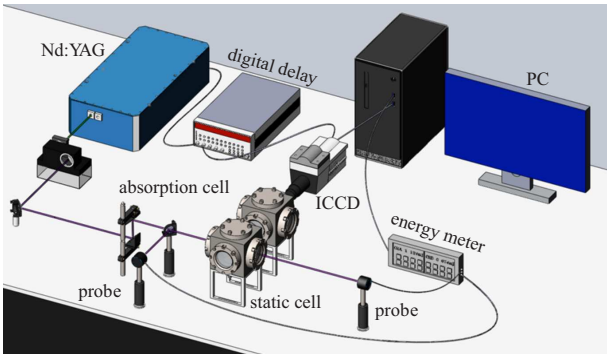


Fig. 3. The schematic diagram of fluorescence's absorption effect.

4. Results and discussion

4.1. Determination of excitation wavelength

Koban[25] and Thurber[22] have studied the absorption spectra of toluene and acetone, respectively. Acetone and toluene have wide absorption ranges in the ultraviolet region. At room temperature, acetone's absorption range is 225 nm to 320 nm and toluene's absorption range is 230 nm to 270 nm. Therefore, the wavelength ranging from 230 nm to 270 nm is the overlap region of acetone and toluene's absorption spectra. According to Thurber[21] and Koch,[30] the FQY of toluene is approximately between 0.1 and 0.3, and the FQY of acetone is approximately between 0.001 and 0.002. Acetone's fluorescence intensity is more dependent on the laser energy than that of toluene. As much laser energy as possible should be used to excite the acetone molecule. The peak of the absorption spectrum of acetone is around 275 nm, so the absorption spectrum range of this experimental study is from 260 nm to 270 nm.

Toluene and acetone's absorption spectra are shown in Figs. 4(a) and 4(b), respectively. The absorption cross-section of toluene is much higher than that of acetone in this wavelength range. The laser wavelength has no obvious influence on the acetone's absorption cross-section. From 260 nm to 270 nm, acetone's absorption cross-section is increased by approximately 1.3 times. The pulsed laser energy has a greater influence on acetone's fluorescence signal intensity than its excitation wavelength, so the wavelength of the high-energy pulsed laser that is easier to obtain is preferred.

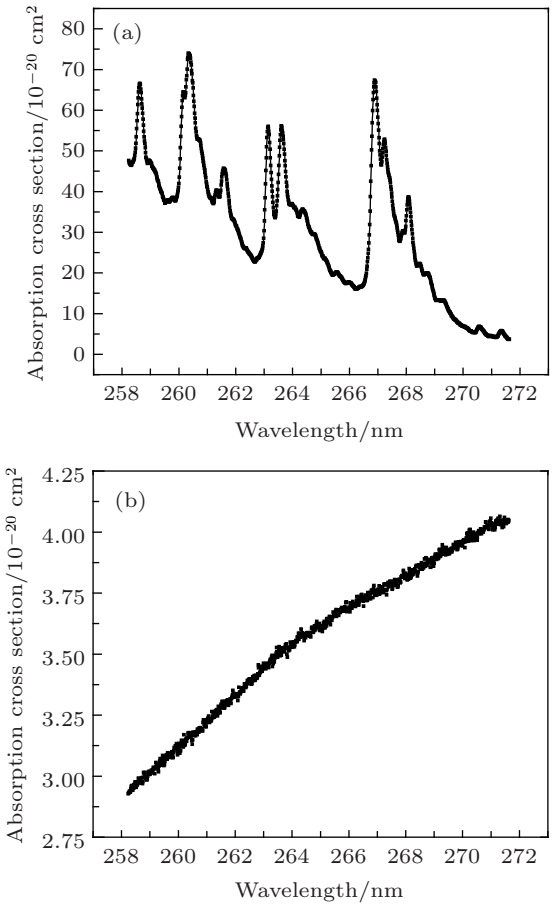


Fig. 4. Absorption spectra of toluene (a) and acetone (b) at room temperature.

The high-energy pulse laser easily obtained in this wavelength range is the 266 nm pulse laser output by the YAG laser used in this experiment. Toluene also has a relatively low absorption cross-section at this laser wavelength, which ensures that more laser energy is used to excite acetone. The absorption cross-sections of acetone and toluene measured with a laser energy meter probe are 4.04×10^{-20} cm^{-2} (σ_a) and 20.35×10^{-20} cm^{-2} (σ_t), respectively. The absorption cross-sections of acetone and toluene measured by Thurber[21] and Koch[30] are 4.4×10^{-20} cm^{-2} and 18×10^{-20} cm^{-2}, respectively. The reason for some differences from the of results Koban[25] and Thurber[22] is that different tracer gas configuration schemes lead to differences in the actual concentration of the tracer, and different laser energy measurement equipment and lasers also affect the final results.

4.2. The filters selection

The experimental device demonstrated in Subsection 3.1 is used to obtain the toluene and acetone's fluorescence spectra in the nitrogen environment to select the appropriate filter according to the spectral characteristics. The fluorescence spectra of acetone and toluene obtained in the static cell under the excitation of a 266 nm pulsed laser are shown in Fig. 5, where each data point has been normalized to its spectral peak value. The fluorescence spectrum peak of toluene is approximately 280 nm, while that of acetone is approximately 450 nm. A Semrock BP280 filter is used to capture the fluorescence signals of toluene, and a Semrock LP430 filter and Andover FL450 filter are used for that of acetone. These methods ensure that the ICCD simply extracts the fluorescence signals, subtracting the noise of the other fluorescence signals and scattered laser light.

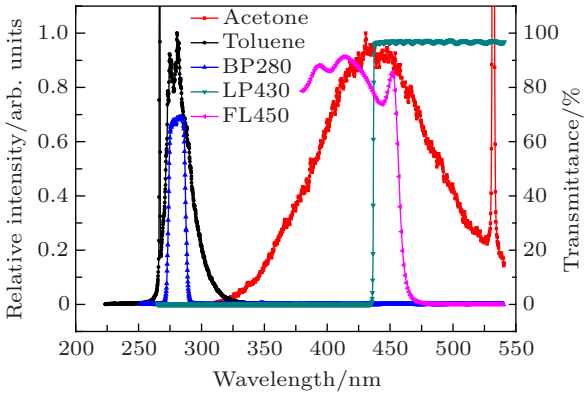


Fig. 5. Fluorescence spectra of acetone (red) and toluene (black) in nitrogen excited at 266 nm and transmission spectrum of the Semrock BP280 (blue), LP430 (green), and Andover FL450 filters (purple).

4.3. The effect of laser energy and tracer concentration

The experimental platform in Subsection 3.1 is used to study the effect of laser energy and tracer concentration on the tracer's fluorescence intensity. Figures 6(a) and 6(b) show the relationship between the intensity of the fluorescent signals of acetone and toluene and the laser energy. The incident laser energy range is 0.1–0.5 mJ. In the experiment, the partial pressures of acetone and toluene are 2 kPa and 1 kPa, the diluent gas is nitrogen, and the total pressure inside the static cell is 101 kPa. Each data point in Fig. 6 is the average value of 40 data points. The experimental results show that in this energy range, the fluorescence signal of acetone and toluene has a good linear relationship with the laser energy. In the following experiment, the energy range of the pulsed laser is always 0.1–0.5 mJ.

Figures 7(a) and 7(b) show the relationship between the fluorescence intensity of acetone and toluene and their respective concentrations. The experimental results show that under a low tracer concentration environment, the concentrations of acetone and toluene have an approximately linear relationship with their respective fluorescence intensity. This is because when the tracer concentration is relatively low, the effect of the molecular collision efficiency's variation on the FQY is not obvious. The approximately linear relationship with corresponding acceptable accuracy can meet the requirement of concentration measurement. In order to maintain this linear relationship, in the following experiments, the concentration range of acetone is 0–10 kPa, and the concentration range of toluene is 0–1.6 kPa. In this tracer concentration range, equa-

tion (5) can be used to achieve a single tracer concentration measurement.

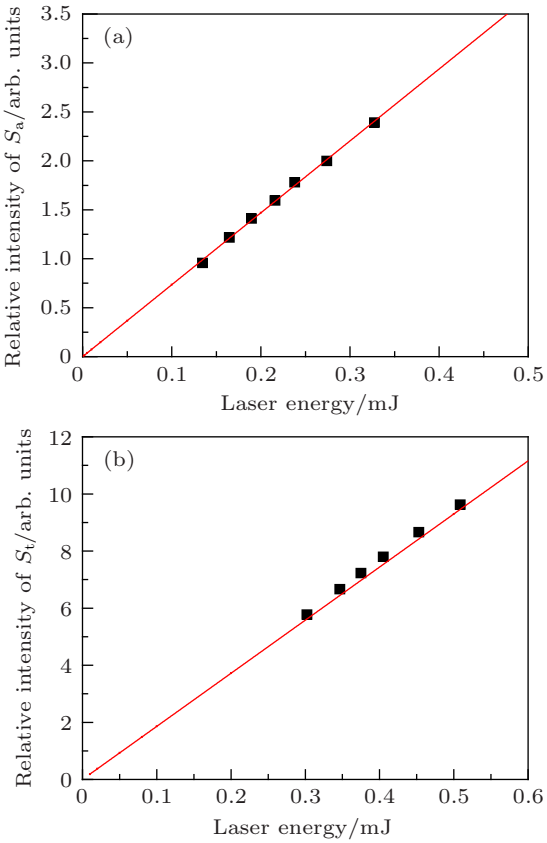


Fig. 6. A linear relationship between acetone (a) and toluene's (b) relative fluorescence intensity and pulsed laser energy.

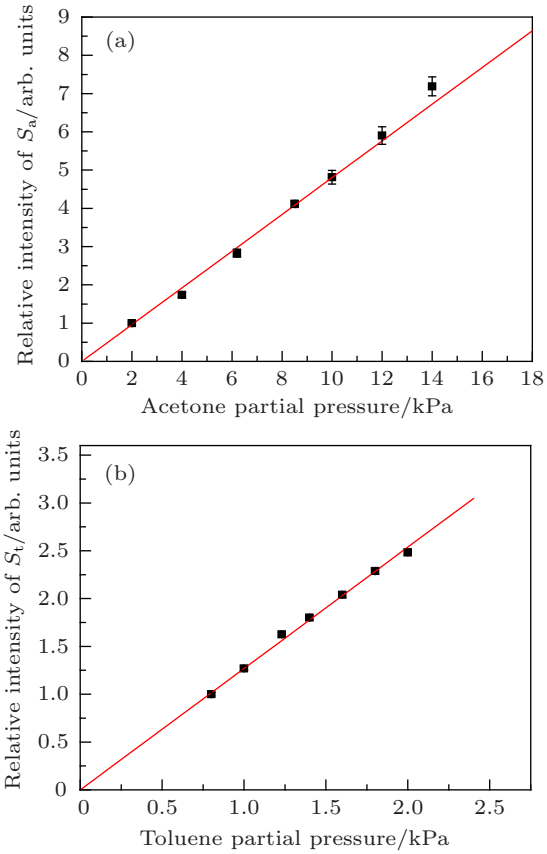


Fig. 7. The relationship between the relative fluorescence intensity of the tracer of acetone (a) and toluene (b) and its concentration.

4.4. The effect of tracers

The next step is to study the absorption effect of acetone and toluene on each other's fluorescence signal using the experimental device described in Fig. 3. Figure 8(a) shows that the variations in toluene's partial pressure in the absorption cell have no obvious effect on acetone's fluorescence intensity, so toluene's absorption effect on acetone's fluorescence signal is negligible. This is because toluene's absorption spectrum and acetone's fluorescence spectrum do not overlap. Instead, acetone has obvious absorption effects on toluene's fluorescence signal as shown in Fig. 8(b). When acetone's partial pressure in the absorption cell reaches 20.9 kPa, toluene's fluorescence signal intensity decreases by 97% compared with that without acetone. This occurs because there is a large overlap between toluene's fluorescence spectrum and acetone's absorption spectrum. According to the length of the absorption path (13 cm) and the partial pressure of acetone, acetone's effective absorption cross-section on toluene's fluorescence signal (σ_{at}) is 5.77×10^{-20} cm^{-2} as calculated using the Lambert–Beer's law at room temperature (296 K). Since the concentration in this experiment is represented by the partial pressure (kPa), the absorption cross-section is equivalent to 0.014 kPa^{-1}.

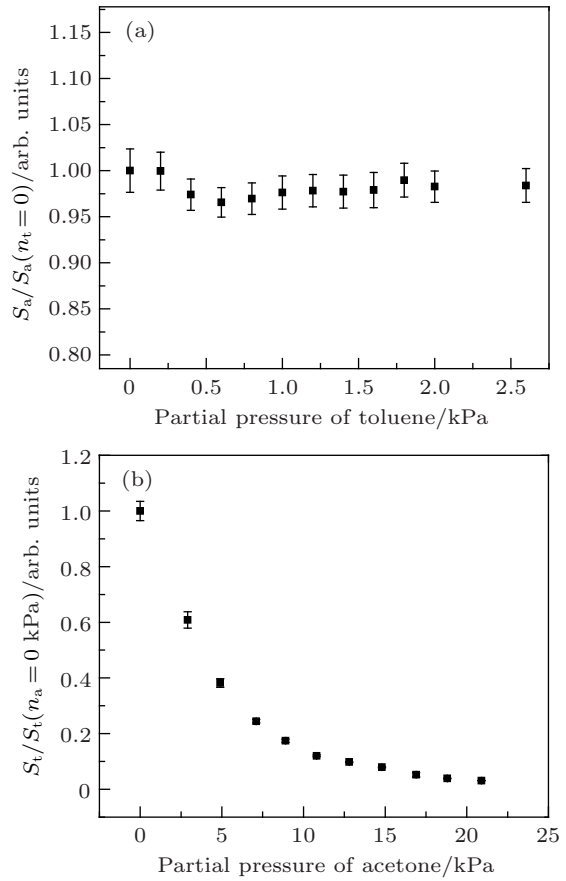


Fig. 8. (a) Toluene's absorption effect on acetone fluorescence signal, (b) acetone's absorption effect on toluene fluorescence signal.

Equations (6) and (7) are further developed into the following ones according to the difference between toluene and acetone:

$$S_{\rm t} = k_{\rm t}E_0\exp(-(\sigma_{\rm a}n_{\rm a}+\sigma_{\rm t}n_{\rm t})x)n_{\rm t}\sigma_{\rm t}\frac{\phi_{\rm t}(n_{\rm a})}{\phi_{\rm t}(n_{\rm a}=0\ {\rm kPa})} \times\exp(-0.014n_{\rm a}L), \quad (10)$$

$$S_{\rm a} = k_{\rm a}E_0\exp(-(\sigma_{\rm a}n_{\rm a}+\sigma_{\rm t}n_{\rm t})x)n_{\rm a}\sigma_{\rm a}\frac{\phi_{\rm a}(n_{\rm t})}{\phi_{\rm a}(n_{\rm t}=0\ {\rm kPa})}, \quad (11)$$

where L is the absorption path length of toluene's fluorescence signal in an acetone vapor environment. In the experiment, using the device in Subsection 3.1, the position of the laser in and out of the static cell is the center of the window, so L in these experiments is 6.5 cm.

The experimental platform in Subsection 3.1 is used to study the quenching and enhancement effects of acetone and toluene on each other's fluorescence signals. Toluene and acetone vapors are filled into the static cells, the partial pressure of toluene vapor is kept at 0.4 kPa, and the variation of toluene's fluorescence signal intensity is observed under different partial pressures of acetone vapor. Based on the known partial pressure and absorption path conditions, the tracers' laser energy is normalized and the influence of the mutual absorption effect can be quantitatively eliminated according to the previously described results, to obtain acetone's effect on toluene's fluorescence signal. Acetone has an obvious quenching effect on toluene's fluorescence signal, as shown in Fig. 9(a). As the acetone's partial pressure increases, the toluene's relative fluorescence intensity gradually decreases. In addition, the working conditions of toluene partial pressures of 0.8 kPa, 1.2 kPa, and 1.6 kPa are studied, and the results are shown in Fig. 9(a). We can find that under the four toluene partial pressures, the acetone's quenching effect on toluene's fluorescence intensity is not significantly different. Figure 9(b) shows that acetone's quenching effect on toluene's fluorescence signals conforms to the Stern–Volmer Eq. (8). The Stern–Volmer factor ($k_{\rm SV}^{\rm ace,tol}$) has no obvious variation with toluene's partial pressure, which shows that the acetone's quenching effect on toluene's fluorescence signal is only related to the acetone's concentration. The average of the four $k_{\rm SV}^{\rm ace,tol}$ in the experiment is 0.50 kPa^{-1}. The following equation is obtained:

$$\frac{I}{I_0} = \frac{1}{0.5n_{\rm a}+1} = \frac{\phi_{\rm t}(n_{\rm a})}{\phi_{\rm t}(n_{\rm a}=0\ {\rm kPa})}, \quad (12)$$

which is $\phi_{\rm t}(n_{\rm a})/\phi_{\rm t}(n_{\rm a}=0\ {\rm kPa})$ of Eq. (10).

The same method is used to study the toluene's effect on acetone's fluorescence signal. The molecular collisions between acetone and toluene not only quench the toluene's fluorescence signal, but also enhance the acetone's fluorescence signal. As shown in Fig. 10(a), acetone's fluorescence signal increases as toluene's partial pressure increases and the growth rate ($k_{\rm G}^{\rm tol,ace}$) is also related to acetone's partial pressure. According to Eq. (9), we can find that $k_{rmG}^{\rm tol,ace}$ decreases as acetone's partial pressure increase as shown in Fig. 10(b). This shows that with the increase of the acetone concentration, toluene's ability to enhance the acetone's relative fluorescence intensity ($k_{\rm G}^{\rm tol,ace}$) is gradually weakened. $k_{\rm G}^{\rm tol,ace}$ and acetone's concentration have an exponential function relationship, as shown in Fig. 11. The following equation is obtained for $\phi_{\rm a}(n_{\rm t})/\phi_{\rm a}(n_{\rm t}=0\ {\rm kPa})$ in Eq. (11):

$$\frac{I}{I_0} = \exp(0.009n_{\rm a}^2-0.205n_{\rm a}+1.011)n_{\rm t}+1 = \frac{\phi_{\rm a}(n_{\rm t})}{\phi_{\rm a}(n_{\rm t}=0\ {\rm kPa})}. \quad (13)$$

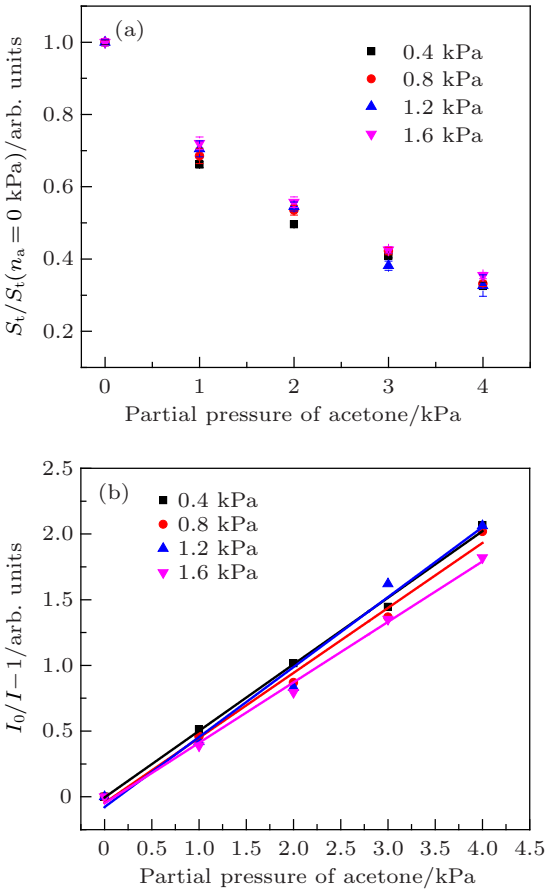


Fig. 9. The quenching effect (a) and Stern–Volmer plots (b) of acetone on toluene's fluorescence intensity at different toluene partial pressures.

In the study of toluene/3-pentanone PLIF technology, Koban[31] found that 3-pentanone significantly quenches the toluene's fluorescence signal. Molecular collisions also lead to the singlet energy transfer from aromatic hydrocarbons to the ketone, enhancing 3-pentanone's fluorescence intensity. Bayrakceken[32] studied the intermolecular collisional energy transfer (IMCET) process, verified that this process is a radiation-less energy transfer from donor's singlet to acceptor's singlet, and labeled this behavior as sensitized fluorescence. He summarized some characteristics of acceptors and donors: 1) for the energy of the first singlet excited state $E_{\rm S1}$,

E_{S1}(donor) is larger than E_{S1}(acceptor), where the overlap of donor emission and acceptor absorption occurs; 2) the donor fluorescence is quenched and the acceptor fluorescence is sensitized. Acetone and toluene satisfy these acceptor and donor characteristics, respectively. The enhancement of the acetone fluorescence signal is a sensitized fluorescence phenomenon. The collision between the excited toluene molecules and the acetone molecules causes the singlet energy to be transferred from toluene to acetone, and the acetone is excited and emits a fluorescent signal.

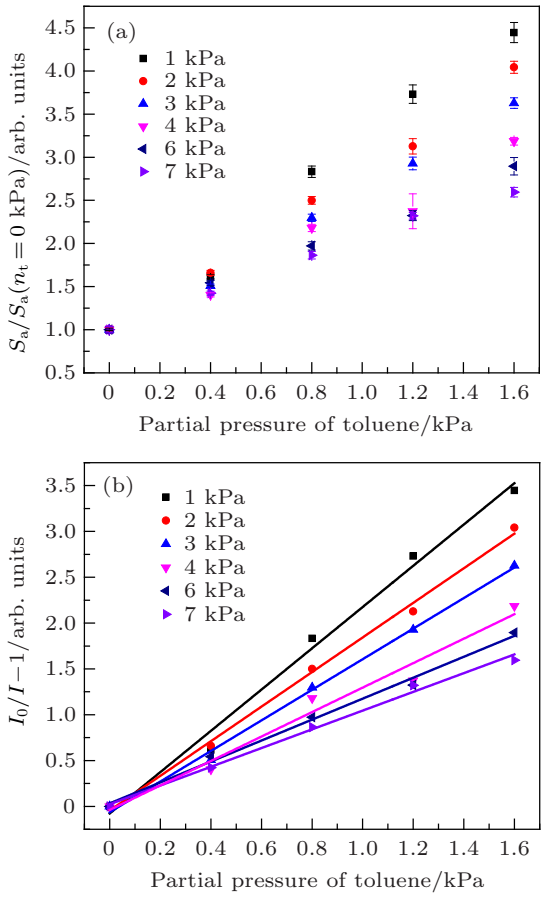


Fig. 10. (a) Acetone's relative fluorescence intensity at different toluene partial pressures, (b) the $k_G^{tol,ace}$ plots of acetone's fluorescence at different acetone partial pressures.

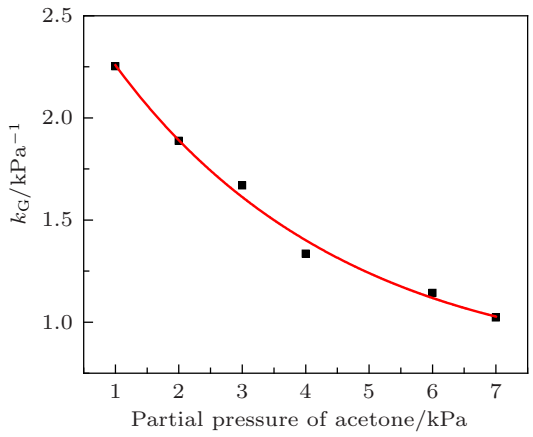


Fig. 11. The $k_G^{tol,ace}$ at different acetone partial pressure.

4.5. Photophysical model for acetone/toluene LIF

According to the experimental phenomenon of the above experiment and the single tracer photophysical model previously studied by Koban[26] and Thurber,[21] a photophysical model of acetone/toluene is established to explain the physical process. The simplified model is illustrated in Fig. 12 through the use of a Jablonski diagram.

The electrons in the ground state (S) of the two tracer molecules are excited by the incident laser energy and leap to the excited state (S_1). Some of these electrons transit to the lower excited state due to vibrational relaxation, then emit fluorescence signals and return to the ground state. This transition mode is a radiative transition. Electrons with different energy levels in the excited states also jump to triplet states (T_1) via intersystem transition (ISC) or to the ground state by internal conversion (IC). The electrons will eventually return to the ground state via the IC and the ISC. These two transition modes are non-radiative transitions. The collisions of acetone and toluene molecules have a quenching effect on the toluene's fluorescence signal, and the excited toluene electrons transit to the triplet state via the ISC or directly return to the ground state. The collision of molecules results in the singlet energy transfer (SET) from toluene molecules to acetone molecules, sensitized fluorescence occurs in acetone, which enhances acetone's fluorescence signal. Due to the overlap between toluene's fluorescence spectrum and acetone's absorption spectrum, part of the toluene's fluorescence signal is absorbed by acetone.

In Subsections 4.3 and 4.4, we conducted a quantitative study on the changes in fluorescence intensity caused by each physical process in the photophysical model. By summarizing these studies, we can establish a quantitative relationship between acetone and toluene's fluorescence intensity and their respective concentrations, as shown by

$$S_t = k_t E_0 \exp(-(\sigma_a n_a + \sigma_t n_t)x) n_t \sigma_t \frac{\exp(-0.014 n_a L)}{0.5 n_a + 1}, \quad (14)$$

$$S_a = k_a E_0 \exp(-(\sigma_a n_a + \sigma_t n_t)x) n_a \sigma_a (\exp(0.009 n_a^2 - 0.205 n_a + 1.011) n_t + 1). \quad (15)$$

Therefore, by simultaneously capturing the fluorescence intensities of acetone and toluene, simultaneous measurement of the two gas components' concentrations can be achieved.

Equations (14) and (15) apply only to measuring the flow field concentration at room temperature with only nitrogen as the dilute gas. Therefore, they can be used to simultaneously measure the concentration of two components in the flow field of the DLP. However, they are not suitable for flow fields with drastic temperature variations, nor can they apply to flow field measurements when non-nitrogen dilute gases (such as oxygen) are introduced. Under these conditions, the effect of the added non-concentration factors on the fluorescence intensity

must be assessed, and equations (14) and (15) should be optimized to make them suitable for specific flow field concentration measurement. The experimental environment in this study is inside a static cell, and the concentrations of various components are consistent everywhere. Using this technique to measure open flow fields, it is necessary to consider the variation of the excitation laser energy caused by the non-uniform concentration of the flow field.

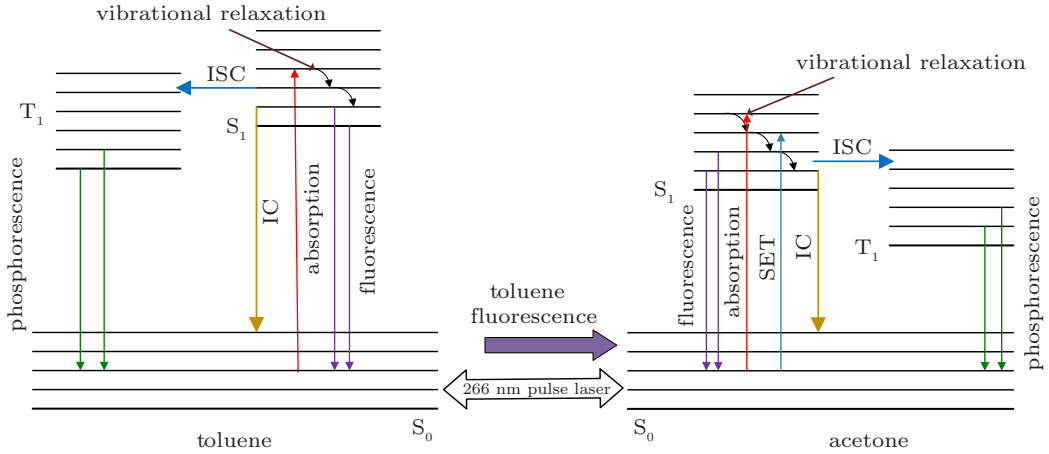


Fig. 12. A simplified model of acetone and toluene's photophysical behavior.

4.6. Uncertainty analysis

Several parameters of Eqs. (14) and (15) are crucial to realize the simultaneous quantitative measurement of two gas components' concentration by acetone/toluene PLIF technology, including the acetone's effective absorption cross-section on toluene's fluorescence signal (σ_{at}), acetone's Stern–Volmer coefficient on toluene's fluorescence signal ($k_{SV}^{ace,tol}$), and toluene's enhancement coefficient on acetone fluorescence signal ($k_G^{tol,ace}$). There will be errors in the three coefficients obtained by measurement and fitting calculation, and the errors mainly come from the measurement errors of the laser energy meter, vacuum gauge, and the ICCD. The measurement experiment of σ_{at} is 5.77×10^{-20} cm^{-2}, and the relative error is 7.1%. $k_{SV}^{ace,tol}$ is 0.50 kPa^{-1}, and the relative error is 6.0%. The specific value of $k_G^{tol,ace}$ is exponentially related to the acetone concentration, and the maximum relative error is 4.7% within the range of the experimentally measured concentration.

5. Conclusion

We propose the simultaneous measurement of the concentration of two components using toluene and acetone dual-tracer PLIF technology. To quantitatively study the effects of acetone and toluene on each other's fluorescence intensity, we choose nitrogen as the only diluent gas, to obtain the quantitative relationship between the tracer's fluorescence intensity and concentration. The experimental results show that acetone has a significant absorption effect on the fluorescence signal emitted by toluene, the effective absorption cross-section is 5.77×10^{-20} cm^{-2}. Acetone has an obvious de-excitation effect on the excited toluene molecules, and the Stern–Volmer coefficient is 0.50 kPa^{-1}. In the same molecular collision process, the toluene's energy of the singlet excited state will be transferred to the acetone molecule, acetone's fluorescence signal intensity is enhanced, and the enhancement coefficient is exponential with the acetone's concentration. The quantitative relationship between the fluorescence intensity of acetone and toluene and the two tracers' concentrations is the theoretical basis for the simultaneous quantitative measurement of two gases' concentrations by using acetone/toluene PLIF technology. A photophysical empirical model is established to explain the fluorescence signals' intensity variations. The next main work is to apply the acetone/toluene PLIF technology to achieve synchronous quantitative measurement of two gas components' concentration in the DLP flow field. Relevant experimental results will be published in the subsequent papers.

References

[1] Sun P, Yuan Y, Ge B, Tian Y, Zhang Z and Zang S 2017 *Energy & Fuels* **31** 10060
[2] Gamal A M, Ibrahim A H, Ali E-M M, Elmahallawy F M, Abdelhafez A, Nemitallah M A, Rashwan S S and Habib M A 2017 *Energy & Fuels* **31** 1980
[3] Park J, Nguyen T H, Joung D, Huh K Y and Lee M C 2013 *Energy & Fuels* **27** 1643
[4] Xie G, Qi H Y, Li Y H, Feng C and Chen X L 2010 *Proceedings of the Chinese Society of Electrical Engineering* **30** 51 (in Chinese)
[5] Di Benedetto A 2013 *Chemical Engineering Science* **99** 265
[6] Zhao W, Liu L, Shen W, Lyu Y and Qiu P 2019 *Energy & Fuels* **33** 2547
[7] Kang T and Kyritsis D C 2005 *Combustion Science and Technology* **177** 2191
[8] Balusamy S, Cessou A and Lecordier B 2014 *Combustion and Flame* **161** 427
[9] Zhang J and Abraham J 2016 *Combustion and Flame* **163** 461
[10] Wei W, Yu Z, Zhou T and Ye T 2018 *International Journal of Hydrogen Energy* **43** 9036

[11] Nwaboh J A, Werhahn O, Ortwein P, Schiel D and Ebert V 2012 *Measurement Science & Technology* **24** 015202
[12] Gao Y, Zhang Y, Dong C, Ying H and Liu W 2016 *International Symposium on Optoelectronic Technology and Application* **10155** 101552R
[13] Ferioli F, Puzinauskas P V and Buckley S G 2003 *Applied Spectroscopy* **57** 1183
[14] Joshi S, Olsen D B, Dumitrescu C, Puzinauskas P V and Yalin A P 2009 *Applied Spectroscopy* **63** 549
[15] Dou H, Dong L, Zhang L, Jia S and Yin W 2008 *Applied Spectroscopy* **62** 458
[16] Hanson R K, Seitzman J M and Paul P H 1990 *Appl. Phys. B* **50** 441
[17] Yu X, Yang Z, Peng J B, Zhang L, Ma Y F, Yang C B, Li X H and Sun R 2015 *Chin. Phys. B* **24** 114204
[18] Chen S, Su T, Li Z S, Bai H C, Yan B and Yang F R 2016 *Chin. Phys. B* **25** 100701
[19] Lozano A, Yip B and Hanson R K 1992 *Exp. Fluids* **13** 369
[20] Hartwig J, Mittal G, Kumar K and Sung C J 2017 *Appl. Phys. B* **123** 191
[21] Thurber M C and Hanson R K 1999 *Appl. Phys. B* **69** 229
[22] Thurber M C, Grisch F, Kirby B J, Votsmeier M and Hanson R K 1998 *Appl. Opt.* **37** 4963
[23] Koch J D and Hanson R K 2003 *Appl. Phys. B* **76** 319
[24] Modica V, Morin C and Guibert P 2007 *Appl. Phys. B* **87** 193
[25] Koban W, Koch J D, Hanson R K and Schulz C 2004 *Phys. Chem. Chem. Phys.* **6** 2940
[26] Koban W, Koch J D, Hanson R K and Schulz C 2005 *Appl. Phys. B* **80** 777
[27] Faust S, Tea G, Dreier T and Schulz C 2013 *Appl. Phys. B* **110** 81
[28] Zimmermann F P, Koban W, Roth C M, Herten D P and Schulz C 2006 *Chem. Phys. Lett.* **426** 248
[29] Meyer T R, King G F, Martin G C, Lucht R P, Schauer F R and Dutton J C 2002 *Exp. Fluids* **32** 603
[30] Koban W, Koch J D, Hanson R K and Schulz C 2005 *Appl. Phys. B* **80** 147
[31] Koban W, Schorr J and Schulz C 2002 *Appl. Phys. B* **74** 111
[32] Bayrakceken F 2008 *Spectrochimica Acta Part A: Molecular and Biomolecular Spectroscopy* **71** 572